Biology Direct

RESEARCH

Open Access

Exploring the association between osteoporosis and kidney stones: a clinical to mechanistic translational study based on big data and bioinformatics

Di Luo[1], Linguo Xie[1], Jingdong Zhang[1] and Chunyu Liu[1*]

Abstract

Background Osteoporosis and kidney stones share several common pathophysiological risk factors, and their association is well-established. However, previous studies have primarily focused on environmental mediators, such as diet, and the precise mechanism linking these two conditions remains unclear.

Methods The relationship between osteoporosis and kidney stones was analyzed using weighted multivariate logistic regression, employing data from five cycles of the National Health and Nutrition Examination Survey (NHANES) from 2007–2010, 2013–2014, and 2017–2020. Gene expression data from the Gene Expression Omnibus (GEO) microarray database were integrated with machine learning techniques to identify key genes involved in both osteoporosis and kidney stones. Common targets were then identified through the Comparative Toxicogenomics Database (CTD) and GeneCards. GMFA enrichment analysis was performed to identify shared biological pathways. Additionally, drug prediction and molecular docking were employed to further investigate the pharmacological relevance of these targets.

Results Analysis of the NHANES database confirmed a strong association between osteoporosis and kidney stones. Weighted multivariate logistic regression showed that osteoporosis (OR: 1.41; 95% CI 1.11–1.79; $P < 0.001$) and bone loss (OR: 1.24; 95% CI 1.08–1.43; $P < 0.001$) were significantly correlated with an increased risk of kidney stones. Three hub genes—WNT1, AKT1, and TNF—were identified through various analytical methods. GMFA revealed that the mTOR signaling pathway is a key shared pathway. Molecular docking studies further confirmed the pharmacological relevance of these targets, demonstrating strong binding affinity between drugs and the proteins involved, consistent with previous findings.

Conclusion Bone loss is associated with an increased risk of kidney stones. Targeting the mTOR signaling pathway may offer a potential therapeutic approach for treating both osteoporosis and kidney stones.

Keywords Kidney stones, Osteoporosis, Bioinformatics analysis, MTOR signaling pathway, Drug target

Introduction

Osteoporosis and kidney stones, though seemingly unrelated conditions in orthopedics and urology, respectively, share several commonalities in their underlying mechanisms and risk factors. Osteoporosis is a systemic bone disorder characterized by reduced bone mass, impaired

*Correspondence:
Chunyu Liu
liuchunyu@tmu.edu.cn
[1] Department of Urology, Tianjin Institute of Urology, The Second Hospital of Tianjin Medical University, 23 Pingjiang Road, Hexi District, Tianjin 300000, People's Republic of China

bone microarchitecture, increased bone fragility, and a higher risk of fractures [1]. In contrast, kidney stones are crystalline deposits that form in the kidneys and often lead to symptoms such as urinary tract obstruction, pain, and hematuria [2]. Despite their distinct clinical manifestations, recent studies have suggested the possibility of shared genetic or environmental risk factors between these two diseases.

The pathogenesis of osteoporosis is influenced by a variety of factors. Genetic factors play a critical role in determining an individual's bone density and strength, with a family history of the disease conferring an increased risk. Deficiencies in calcium and vitamin D impair bone matrix formation and mineralization. Hormonal factors, particularly deficiencies in estrogen and androgen, promote increased bone resorption and decreased bone formation. With advancing age, the decline in endocrine and digestive system functions further disrupts bone metabolism. Poor lifestyle choices, including lack of physical activity, poor dietary habits, smoking, and excessive alcohol consumption, also contribute to the risk of osteoporosis. Additionally, certain medical conditions and medications can adversely affect bone metabolism [3, 4].

The mechanism underlying kidney stone formation is multifactorial and involves several factors, including urinary component imbalances, reduced inhibitor levels, urinary tract obstruction and infection, metabolic abnormalities, genetic predisposition, and environmental influences [2]. Elevated concentrations of urinary components, such as calcium and oxalate, exceed their solubility limits, leading to crystal precipitation. These crystals gradually increase in size and form stones. Urinary tract obstruction and infections facilitate the attachment and growth of these crystals [2, 5]. Metabolic disorders, such as hypercalciuria, further elevate the risk of stone formation. Genetic factors affect an individual's metabolism and excretion of stone-forming components [6]. Additionally, environmental, dietary, medication, and psychological factors must also be considered [5].

Previous studies have found no direct relationship between kidney stones and osteoporosis but suggest that the two conditions may be indirectly linked in some cases. For instance, certain medications or treatments may affect both the urinary and skeletal systems, thereby influencing the development and progression of both kidney stones and osteoporosis [7]. Additionally, lifestyle factors such as physical inactivity and high-salt diets may increase the risk of both conditions [8, 9]. These findings highlight the potential interaction between kidney stones and osteoporosis, which may concurrently influence the development of both conditions. However, most current research has been conducted from a clinical perspective, with limited investigation into the genetic relationship between kidney stones and osteoporosis.

This study aims to investigate the relationship between osteoporosis and kidney stones by utilizing the National Health and Nutrition Examination Survey (NHANES) database. Additionally, bioinformatics approaches will be employed to elucidate the potential shared mechanisms underlying these two diseases. The NHANES database, managed by the U.S. Department of Health and Human Services (HHS) through the National Center for Health Statistics (NCHS), collects extensive health and nutrition data from a representative sample of participants. This includes physiological measurements, health questionnaires, laboratory tests, and dietary surveys [10]. These data provide a valuable foundation for assessing the health status of the U.S. population and offer a rich resource for studying the relationship between osteoporosis and kidney stones. Bioinformatics techniques enable the analysis of biological macromolecule interaction networks, gene expression regulation, and disease-related molecular markers, thereby offering new insights into the potential links between osteoporosis and kidney stones. This study aims to uncover the underlying biological links between osteoporosis/osteopenia and kidney stones, providing a scientific basis for early diagnosis, personalized treatment, and the development of prevention strategies. Additionally, it will enhance our understanding of the pathophysiological mechanisms of the skeletal and urinary systems, thereby advancing both basic research and clinical applications in related fields. The research flowchart for this study is presented in Fig. 1.

Methods

The relationship between osteoporosis/osteopenia and kidney stones based on the NHANES database

Study population in NHANES

The data used in this analysis are publicly available through the NHANES database (https://www.cdc.gov/nchs/nhanes/index.htm). The NHANES study protocol was approved by the National Center for Health Statistics (NCHS), and informed consent was obtained from all participants. Institutional review board approval was not required as the study utilized de-identified, publicly available data. A total of 64,929 participants were selected from five cycles: 2007–2010, 2013–2014, and 2017–2020. Participants younger than 20 years of age, as well as those with missing data on kidney stones, bone density, or BMI, were excluded. Ultimately, 13,357 participants were included in the final analysis (Supplementary Fig. 1).

Kidney stones

For participants aged ≥ 20 years, personal interview data on the history of kidney stones were provided in the

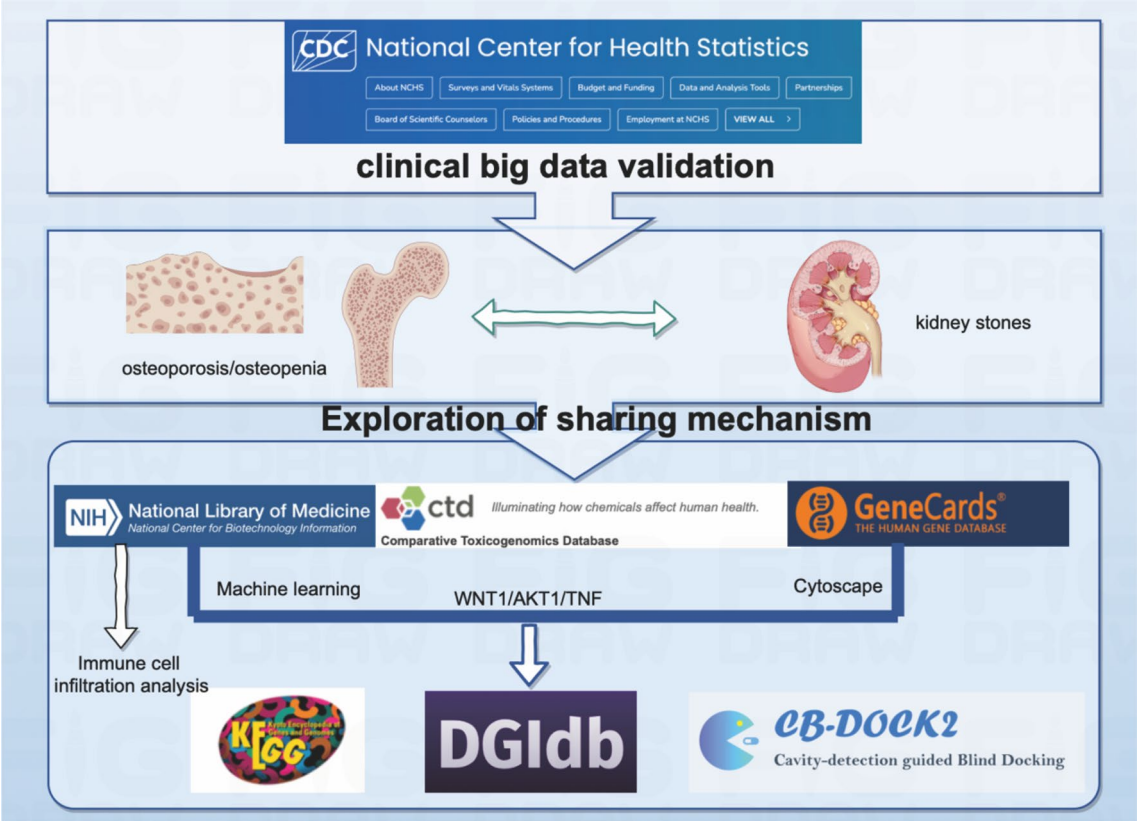

Fig. 1 Graphical workflow of this study. Identification of the workflow for exploring the association between osteoporosis and kidney stones, analysis of the databases, software, and tools used

NHANES 2007–2010, 2013–2014, 2017–2020 (Kidney Conditions–Urology). As described by a previous study, participants who answered "Yes" to the question "Have you ever had kidney stones?" (KIQ026) were defined as KSD. The validity of self-reported kidney stones has been confirmed by previous studies [11].

Measurement of BMD

Bone mineral density (BMD) of the femur and lumbar spine was assessed using dual-energy X-ray absorptiometry (DXA). Osteoporosis was defined as a T-score of < -2.5, while osteopenia was defined as a T-score between -1.0 and -2.5, following the criteria established by Looker et al. In the present study, decreased bone mass was defined as BMD values 1 to 2.5 standard deviations (SD) below the mean for males and females aged 20 to 29 years. Osteoporosis was defined as BMD values more than 2.5 SD below the reference mean for young adults [12, 13].

Other covariates used in NHANES

To control for potential confounding factors, the following demographic characteristics were adjusted for: gender, age, race, education level, body mass index (BMI), smoking status, alcohol consumption, hypertension, and diabetes status. Information on smoking, alcohol use, hypertension, and diabetes status were obtained from the questionnaire responses, while BMI data was derived from the BMXBMI item. All other demographic information was extracted from the demographics section of the NHANES dataset. The dietary intake data were obtained from the 24-h dietary recall interview (Dietary Interview—Total Nutrient Intakes, First Day). The US Department of Food and Nutrient Database for Dietary Studies (FNDDS) was used to calculate the dietary intakes. In the current study, dietary intakes selected as dependent variables for analysis included calcium, phosphate, magnesium, and vitamin D (a total of 25OHD2 and 25OHD3).

The relationship between osteoporosis and kidney stones based on bioinformatics research

Identification of common genes through DEGs analysis

We conducted a differential gene expression (DEG) analysis on the normalized GSE73680 and GSE56815 datasets using the "limma" package in R software. We selected the following thresholds after considering a combination of

gene expression levels, statistical significance, and biological significance. For the GSE73680 dataset, differentially expressed genes (DEGs) were identified with $|\log FC| \geq 1$ and a p value < 0.05, while for the GSE56815 dataset, the thresholds were set at $|\log FC| \geq 0.2$ and p value < 0.05. The DEGs were visualized using volcano plots and heatmaps. Next, upregulated and downregulated genes from both datasets were intersected to identify co-expressed genes. To pinpoint key co-expressed genes associated with KSD and OP, we applied two machine learning algorithms, Lasso and Boruta, to select the most critical core genes.

Shared gene targets obtained from public database

Venn diagrams were employed to identify genes related to osteoporosis/bone loss and kidney stones that are shared between two public databases, CTD and GeneCards. The intersection of these gene sets was then analyzed to identify common gene targets between osteoporosis/bone loss and kidney stones. A protein–protein interaction (PPI) network was constructed using the Search Tool for the Retrieval of Interacting Genes (STRING; http://string-db.org). Key target genes were selected using the CytoHubba plugin in Cytoscape software, complementing the results of the machine learning algorithm.

Analysis of immune cell infiltration

Immune cells display distinct filtering and retention patterns during disease onset and progression. These patterns offer valuable insights into their roles in disease mechanisms and are crucial for the development of novel therapeutic strategies. CIBERSORT, based on linear support vector regression (SVR), estimates the relative abundance of individual immune cell subpopulations in a mixed-cell sample. It achieves this by training on gene expression profiles that are specific to immune cell types. We present the results of immune cell infiltration and associated features using box plots, stacked histograms, and correlation heatmaps.

Candidate drug prediction

Evaluating protein-drug interactions is crucial for determining whether a target protein is a viable candidate for drug development. In this study, we utilized the Drug Signature Database (DSigDB, http://dsigdb.tanlab.org/DSigDBv1.0/) to achieve this objective. DSigDB contains data on 22,527 genes and 17,389 distinct compounds, covering 19,531 genes, making it a comprehensive resource for linking drugs and other compounds to their target genes. Specifically, we uploaded the genomorphic results of screened target proteins to DSigDB, enabling the prediction of drug candidates that interact with these target genes, thus facilitating the goal of targeted gene therapy.

Molecular docking

To further investigate the effects of drug candidates on target proteins and assess the drug availability of these targets, this study performed molecular docking simulations at the atomic level to evaluate the binding affinity and interaction patterns between the drugs and their targets. Molecular docking allows for the analysis of ligand-receptor binding affinity and interaction dynamics. By identifying ligands with high binding affinity and favorable interaction profiles, we can prioritize drug targets for experimental validation and optimize the design of potential drug candidates. The 2D chemical structures of the drugs were retrieved from the PubChem database (https://pubchem.ncbi.nlm.nih.gov), and the protein crystal structures were obtained from the Protein Data Bank (PDB, https://www.rcsb.org/). Molecular docking simulations were conducted using the CB-Dock2 platform (https://cadd.labshare.cn/cb-dock2/php/index.php).

Statistical analysis

For the NHANES analysis, multivariable-adjusted logistic regression was performed to assess the associations between osteoporosis, bone loss, femoral neck BMD, lumbar spine BMD, and KSD. We assessed multicollinearity between variables using Variance Inflation Factor (VIF) before performing multivariate logistics regression analysis. Three models were evaluated, each correcting for different sets of covariates: Model 1 was unadjusted; Model 2 adjusted for sex, age, ethnicity, education level, and BMI; and Model 3 further adjusted for smoking, alcohol consumption, hypertension, diabetes mellitus, Vitamin D, Calcium, Phosphorus and Magnesium in addition to the covariates in Model 2. Results are presented as odds ratios (OR) with 95% confidence intervals (95% CI). Due to the complex probabilistic sampling design of NHANES, weights were incorporated into the statistical analysis. For gene screening, Lasso regression and the Boruta algorithm were employed. Lasso regression is particularly suited for linear relationships and situations where the number of variables exceeds the number of samples, while the Boruta algorithm focuses on feature importance and automated feature selection. This study combines the strengths of both methods. All statistical analyses were conducted using R software version 4.3.2 (R Foundation, Vienna, Austria).

Results

Population characteristics of study subjects according to Kidney stones

A total of 13,357 patients participated in the study. The thresholds for osteoporosis in men were defined as femoral neck (FN) BMD below 0.609 g/cm^2, lumbar spine L1 BMD below 0.692 g/cm^2, L2 BMD below 0.756 g/cm^2, L3 BMD below 0.759 g/cm^2, and L4 BMD below 0.754 g/cm^2. The thresholds for bone loss in the femoral neck and L1-L4 lumbar vertebrae in men ranged from 0.609–0.825 g/cm^2, 0.692–0.876 g/cm^2, 0.756–0.946 g/cm^2, 0.759–0.952 g/cm^2, and 0.754–0.944 g/cm^2, respectively. In women, the thresholds for osteoporosis were FN BMD below 0.551 g/cm^2, L1 BMD below 0.640 g/cm^2, L2 BMD below 0.744 g/cm^2, L3 BMD below 0.783 g/cm^2, and L4 BMD below 0.784 g/cm^2. The thresholds for bone loss in the femoral neck and L1-L4 lumbar vertebrae in women ranged from 0.551–0.756 g/cm^2, 0.640–0.832 g/cm^2, 0.744–0.936 g/cm^2, 0.783–0.973 g/cm^2, and 0.784–0.965 g/cm^2, respectively (Table 1). Table 2 presents the clinical and laboratory characteristics of the study participants. The participants were divided into two groups: 1243 individuals with kidney stones and 12,114 without. Compared to those without kidney stones, individuals in the kidney stone group were older, predominantly male, and of non-Hispanic white descent. Additionally, they had lower educational attainment, higher rates of smoking and alcohol consumption, and a greater prevalence of diabetes and hypertension.

Observational associations between osteoporosis/osteopenia and KSD in NHANES

Univariate analysis revealed that patients with renal stones had lower femoral neck bone mineral density (BMD) (0.78 ± 0.14 vs. 0.81 ± 0.16), as well as a higher prevalence of bone loss (54.7% vs. 48.5%) and osteoporosis (10.4% vs. 8.5%) compared to those without renal stones. However, no significant differences were observed in lumbar spine BMD at L1-L4 between the two groups. Upon stratification by gender, we found that lumbar spine BMD was lower in the kidney stone group among female patients (Supplementary Table 1). The Variance Inflation Factor (VIF) analysis revealed the absence of notable multicollinearity among the remaining covariates, with the exception of data pertaining to bone mineral density. Consequently, we delved into the correlation between bone mineral density at various anatomical sites concurrently and the incidence of kidney stones (Supplementary Fig. 2). Subsequent multifactorial analyses identified a significant negative association between BMD and the prevalence of kidney stones. Patients with osteopenia and osteoporosis, specifically, exhibited a higher risk of developing kidney stones (Table 3). In model 3, adjusted for all covariates, femoral neck BMD (OR = 0.35; 95% CI = 0.18–0.68, P = 0.002), L1 BMD (OR = 0.43; 95% CI = 0.25–0.74, P = 0.002), L2 BMD (OR = 0.47; 95% CI = 0.28–0.78, P = 0.004), L3 BMD (OR = 0.49; 95% CI = 0.30–0.80, P = 0.005), and L4 BMD (OR = 0.48; 95% CI = 0.29–0.78, P = 0.003) were all inversely associated with the risk of kidney stones. The prevalence of kidney stones was higher in patients with reduced bone mass (OR = 1.24; 95% CI = 1.08–1.43, P = 0.002) and

Table 1 Mean femoral bone mineral density (BMD) of 20–29-year-old men and women in NHANES 2007–2010, 2013–2014, and 2017–2020

Region of interest	Mean (gm/cm^2)	SD (gm/cm^2)	BMD cutoff values for	
			Osteopenia	Osteoporosis
Men (n = 766)				
FN BMD	0.969	0.144	0.609–0.825	< 0.609
L1 BMD	0.999	0.123	0.692–0.876	< 0.692
L2 BMD	1.073	0.127	0.756–0.946	< 0.756
L3 BMD	1.081	0.129	0.759–0.952	< 0.759
L4 BMD	1.071	0.127	0.754–0.944	< 0.754
Women (n = 674)				
FN BMD	0.893	0.137	0.551–0.756	< 0.551
L1 BMD	0.960	0.128	0.640–0.832	< 0.640
L2 BMD	1.064	0.128	0.744–0.936	< 0.744
L3 BMD	1.100	0.127	0.783–0.973	< 0.783
L4 BMD	1.086	0.121	0.784–0.965	< 0.784

For each of the four regions of interest, low bone density was defined as: (1) osteopenia: a BMD value between 1 standard deviation (SD) and 2.5 SD below the mean of men or women age 20–29 years; and (2) osteoporosis: a BMD value > 2.5 SD below the young reference mean

Table 2 Patient demographics and baseline characteristics

Characteristic	Non-kidney stones (*N* = 12,114)	Kidney stones (*N* = 1243)	*p* value
Age, years	52 ± 16	57 ± 14	< 0.001[1]
Gender, %			
Male	5756 (47.5%)	709 (57.0%)	< 0.001[2]
Female	6358 (52.5%)	534 (43.0%)	
BMI, kg/m^2	28.1 ± 5.8	29.3 ± 5.7	< 0.001[1]
Race/Ethnicity, %			
Mexican American	2004 (16.5%)	167 (13.4%)	< 0.001[2]
Other hispanic	1348 (11.1%)	150 (12.1%)	
Non-hispanic white	4815 (39.7%)	654 (52.6%)	
Non-hispanic black	2556 (21.1%)	181 (14.6%)	
Other	1391 (11.6%)	91 (7.3%)	
Education level, %			
Less than 9th grade	1282 (10.6%)	133 (10.7%)	< 0.001[2]
9–11th grade	1704 (14.1%)	148 (11.9%)	
High school or equivalent	2876 (23.7%)	287 (23.1%)	
Some college or AA degree	3411 (28.2%)	407 (32.7%)	
College graduate or above	2826 (23.4%)	268 (21.6%)	
Diabetes, %			
Yes	1569 (13.0%)	279 (22.4%)	< 0.001[2]
No/borderline	10,545 (87.0%)	964 (77.6%)	
Hypertensive, %			
Yes	4246 (35.1%)	616 (49.6%)	< 0.001[2]
No	7868 (64.9%)	627 (50.4%)	
Smoke, %			
Yes	5236 (43.2%)	592 (47.6%)	0.003[2]
No	6878 (56.8%)	651 (52.4%)	
Alcohol consumption, cup	2.00 (1.00, 3.00)	2.00 (1.00, 3.00)	< 0.001[3]
FNBMD, gm/cm^2	0.81 ± 0.16	0.78 ± 0.14	< 0.001[1]
L1BMD, gm/cm^2	0.95 ± 0.16	0.95 ± 0.17	0.559[1]
L2BMD, gm/cm^2	1.02 ± 0.17	1.01 ± 0.17	0.226[1]
L3BMD, gm/cm^2	1.05 ± 0.17	1.04 ± 0.17	0.189[1]
L4BMD, gm/cm^2	1.05 ± 0.17	1.04 ± 0.17	0.211[1]
Vitamin D (mcg)	3.10 (1.20, 6.00)	3.30 (1.40, 5.60)	0.531[3]
Calcium (mg)	792.00 (506.75, 1157.00)	799.00 (524.00, 1145.00)	0.358[3]
Phosphorus (mg)	1214.00 (869.00, 1657.00)	1202.00 (887.00, 1633.00)	0.998[3]
Magnesium (mg)	269.00 (196.00, 365.00)	261.00 (198.00, 361.00)	0.136[3]
Osteopenia, %	5870 (48.5%)	680 (54.7%)	< 0.001[2]
Osteoporosis, %	1030 (8.5%)	129 (10.4%)	< 0.001[2]

[1] Welch Two Sample *t*-test, [2]Pearson's Chi-squared test, [3]Wilcoxon rank sum test

osteoporosis (OR = 1.41; 95% CI = 1.11–1.79, $P = 0.005$) (Table 3).

Restricted cubic spline plots were used to assess the dose–response relationship between bone mineral density (BMD) and the risk of kidney stones. Our analysis revealed a significant inverse association between BMD and the risk of kidney stones. This association remained consistent when stratified by sex. In the female group, femoral neck (FN) BMD, L2 BMD, and L4 BMD exhibited a linear negative association with the risk of kidney stones, whereas nonlinear negative associations were observed in the male group and across the entire population (Fig. 2).

Identification of DEGs in KSD and OP

After normalizing the required datasets, we identified a total of 1651 differentially expressed genes in the KSD

Table 3 Logistic regression analysis of BMD and kidney stone

Variables	Model 1		Model 2		Model 3	
	OR (95%CI)	*P*	OR (95%CI)	*P*	OR (95%CI)	*P*
FN BMD	0.32 (0.22 ~ 0.48)	**< 0.001**	0.36 (0.21 ~ 0.60)	**< 0.001**	0.35 (0.18 ~ 0.68)	**0.002**
L1 BMD	0.90 (0.63 ~ 1.28)	0.548	0.54 (0.36 ~ 0.82)	**0.003**	0.43 (0.25 ~ 0.74)	**0.002**
L2 BMD	0.80 (0.56 ~ 1.14)	0.216	0.57 (0.39 ~ 0.85)	**0.006**	0.47 (0.28 ~ 0.78)	**0.004**
L3 BMD	0.79 (0.55 ~ 1.12)	0.179	0.58 (0.40 ~ 0.84)	**0.004**	0.49 (0.30 ~ 0.80)	**0.005**
L4 BMD	0.80 (0.57 ~ 1.13)	0.206	0.53 (0.37 ~ 0.77)	**< 0.001**	0.48 (0.29 ~ 0.78)	**0.003**
Osteopenia	1.39 (1.23 ~ 1.58)	**< 0.001**	1.25 (1.08 ~ 1.43)	**0.002**	1.24 (1.08 ~ 1.43)	**0.002**
Osteoporosis	1.50 (1.22 ~ 1.85)	**< 0.001**	1.39 (1.09 ~ 1.77)	**0.007**	1.41 (1.11 ~ 1.79)	**0.005**

Results with significant differences are shown in bold

Model 1: unadjusted

Model 2: adjusted for age, gender, race/ethnicity, education level and BMI

Model 3: further adjusted for diabetes, hypertensive, smoke, alcohol consumption, Vitamin D, Calcium, Phosphorus and Magnesium

(See figure on next page.)

Fig. 2 Dose–response relationship analysis between BMD and kidney stone. Restricted cubic spline plots of the association between BMD and kidney stone. RCS regression was adjusted for age, race, sex, marital status, education level, smoking status, drinking status, hypertension, diabetes Vitamin D, Calcium, Phosphorus and Magnesium. (Model 3). The blue solid line represents ORs, blue shaded region represents 95% CI. The *P* value indicates the degree of significant difference between the model and the observed data. The smaller the *P* value, the more significant the difference. The *P* Nonlinear value reflects whether there is a nonlinear relationship in the data. If the *P* Nonlinear value is small, it suggests that a nonlinear relationship may exist. Among all participants, FN BMD (femoral neck bone mineral density) has a nonlinear negative correlation with the prevalence of kidney stones (*P* value ≤ 0.001, *P* Nonlinear = 0.013), L1 BMD (first lumbar vertebra bone mineral density) has a nonlinear negative correlation with the prevalence of kidney stones (*P* value ≤ 0.001, *P* Nonlinear ≤ 0.001), L2 BMD (second lumbar vertebra bone mineral density) has a linear negative correlation with the prevalence of kidney stones (*P* value = 0.018, *P* Nonlinear = 0.164), L3 BMD (third lumbar vertebra bone mineral density) has a linear negative correlation with the prevalence of kidney stones (*P* value = 0.013, *P* Nonlinear = 0.085), and L4 BMD (fourth lumbar vertebra bone mineral density) has a nonlinear negative correlation with the prevalence of kidney stones (*P* value = 0.002, *P* Nonlinear = 0.021). In the male population, FN BMD has a nonlinear negative correlation with the prevalence of kidney stones (*P* value = 0.004, *P* Nonlinear = 0.031), L1 BMD has a nonlinear negative correlation (*P* value ≤ 0.001, *P* Nonlinear ≤ 0.001), L2 BMD has a linear negative correlation (*P* value = 0.017, *P* Nonlinear = 0.075), L3 BMD has a nonlinear negative correlation (*P* value = 0.002, *P* Nonlinear = 0.015), and L4 BMD has a nonlinear negative correlation (*P* value = 0.004, *P* Nonlinear = 0.011). In the female population, FN BMD has a linear negative correlation with the prevalence of kidney stones (*P* value = 0.026, *P* Nonlinear = 0.731), L1 BMD has a nonlinear negative correlation (*P* value = 0.001, *P* Nonlinear = 0.003), L2 BMD has a linear negative correlation (*P* value = 0.063, *P* Nonlinear = 0.699), L3 BMD has a linear negative correlation (*P* value = 0.075, *P* Nonlinear = 0.137), and L4 BMD has a linear negative correlation with the prevalence of kidney stones (*P* value = 0.017, *P* Nonlinear = 0.996)

dataset (GSE73680), including 1548 upregulated genes and 103 downregulated genes. Similarly, 1651 differentially expressed genes were identified in the OP dataset (GSE56815), comprising 840 upregulated genes and 811 downregulated genes. Volcano and heatmap analyses revealed the differential expression patterns of genes in both the KSD and OP datasets (Fig. 3A-D). Further intersection analysis identified 14 co-expressed genes, including 9 commonly upregulated genes (WNT1, BTN2A1, MPZ, ACTN2, KLK3, ONECUT2, CRB1, ATMIN, CHI3L1) and 5 commonly downregulated genes (FLNA, RECK, KANK2, RAMP1, ACTA2) (Fig. 3E-F). We employed two machine learning algorithms, Lasso and Boruta, to identify the most critical core genes, ultimately pinpointing WNT1 as the key gene for both KSD and OP (Fig. 4A-G).

Analysis of common gene targets from two public databases

To integrate the existing biological data, we searched for relevant genes in the CTD and GeneCards databases using "osteoporosis/osteopenia" and "kidney stone" as keywords. We then combined the osteoporosis/osteopenia- and kidney stone-related genes from these databases using Venn diagrams, identifying 267 common gene targets, indicating a substantial overlap between osteoporosis/osteopenia and kidney stone (Fig. 5A-B). Subsequently, we conducted core target screening with the Centiscape 2.2 plugin in Cytoscape, integrating the MCC, MNC, Radiality, Stress, BottleNeck, and EcCentricity

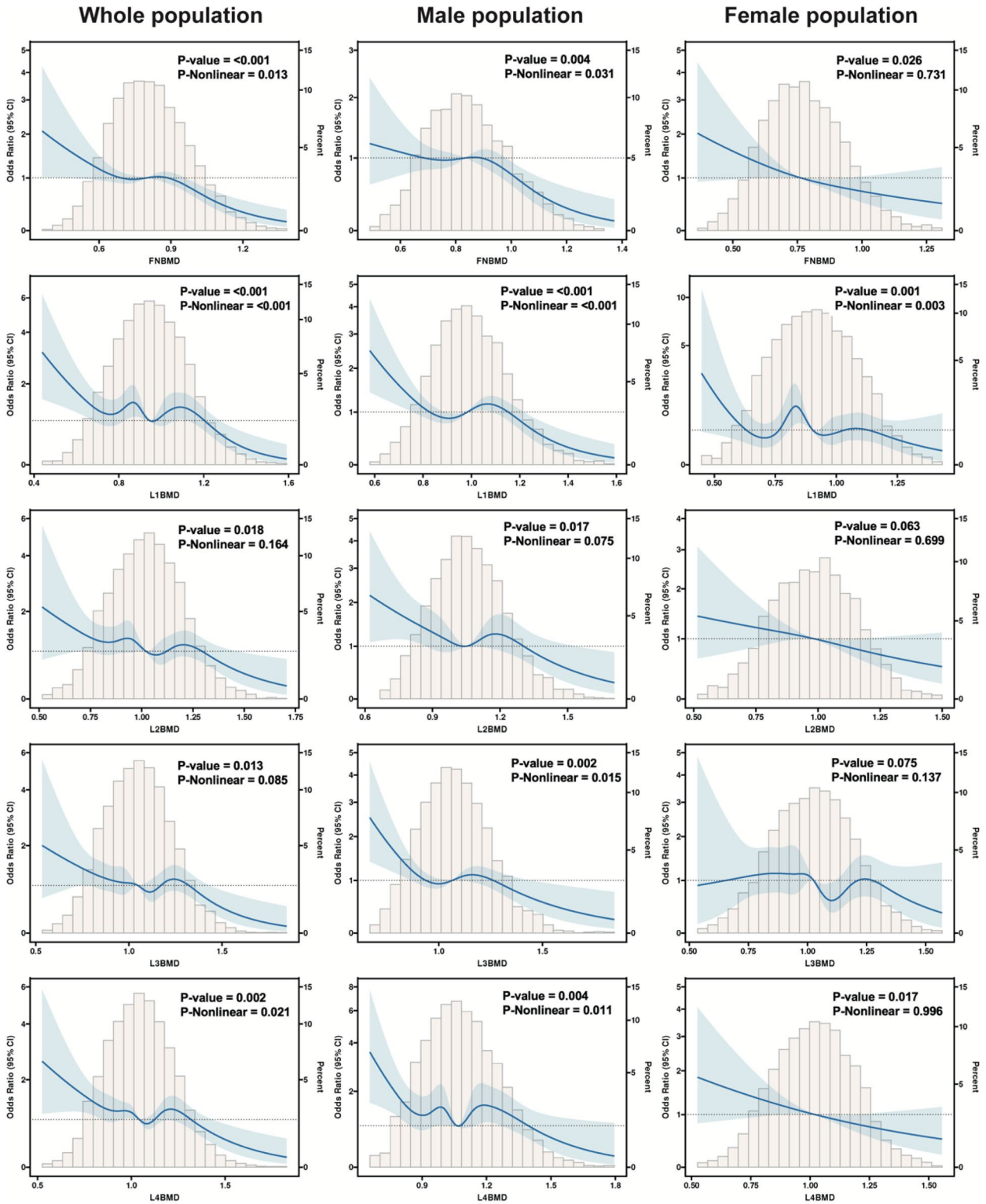

Fig. 2 (See legend on previous page.)

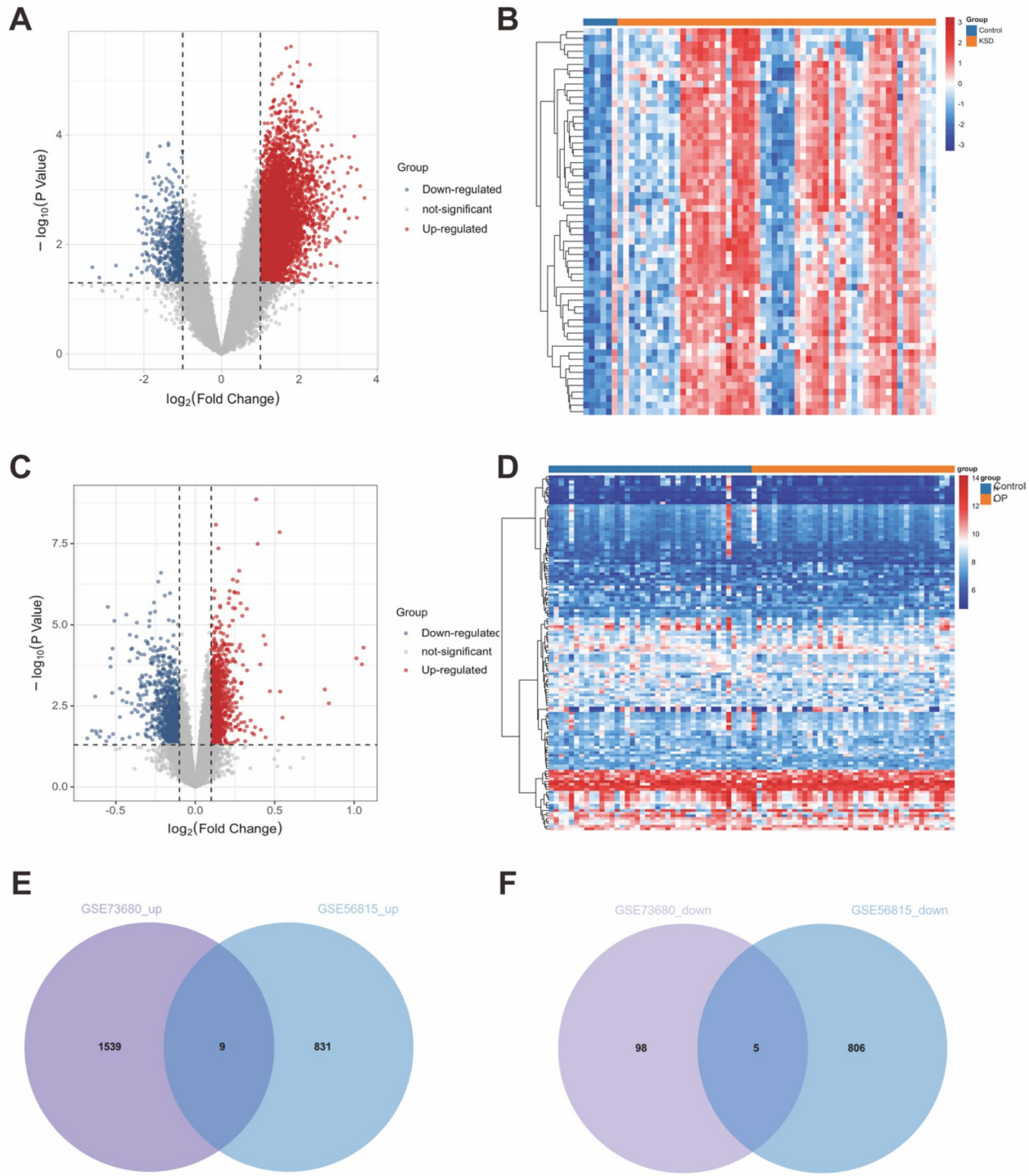

Fig. 3 Differential gene expression analysis. **A** Volcano plots depict the differential expression genes (DEGs) in GSE73680. **B** Heatmaps illustrate the expression patterns of corresponding DEGs in GSE73680. **C** Volcano plots depict the DEGs in GSE56815. **D** Heatmaps illustrate the expression patterns of corresponding DEGs in GSE56815. **E** Co-up-regulated genes in GSE73680 and GSE56815. **F** Co-down-regulated genes in GSE73680 and GSE56815

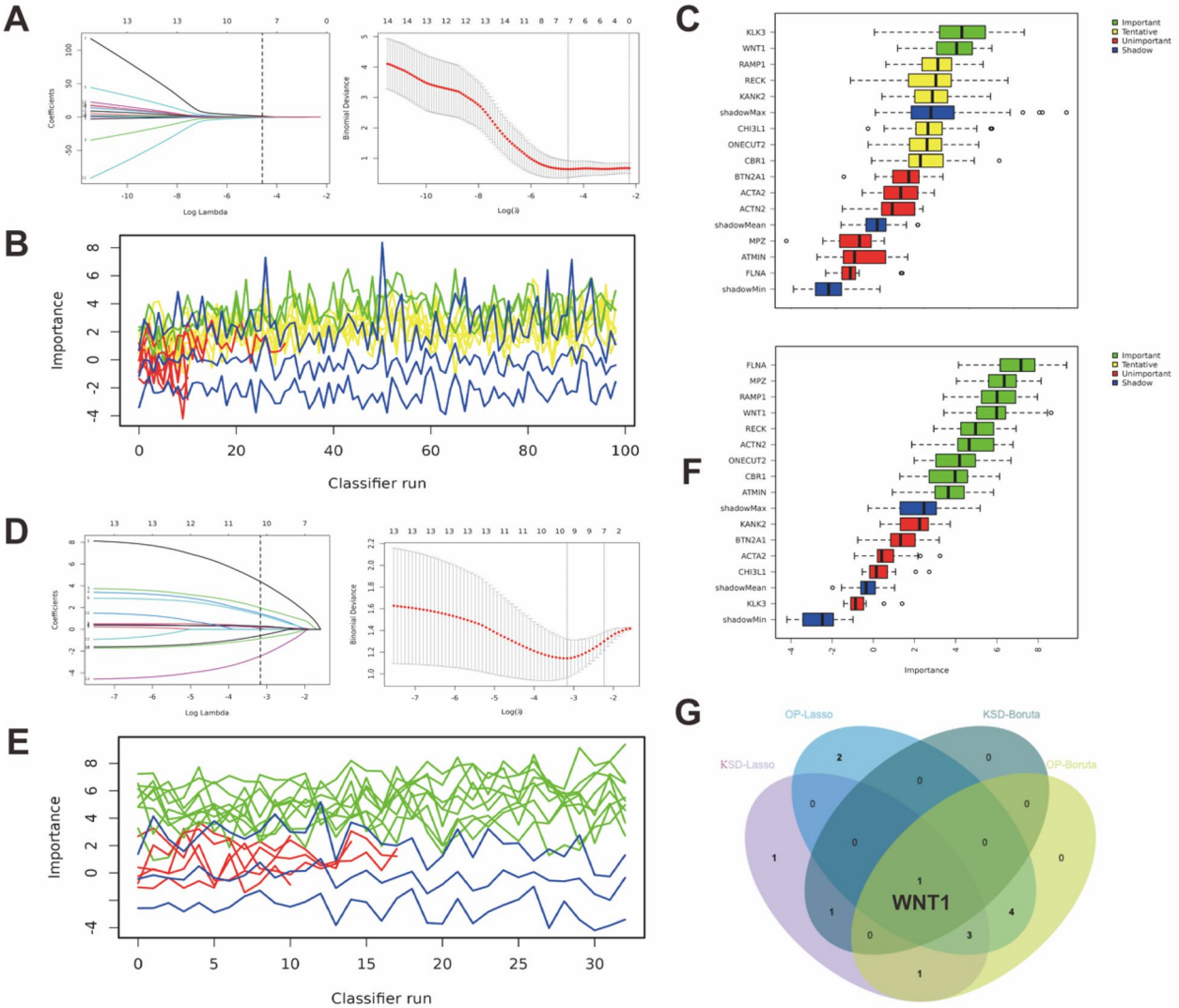

Fig. 4 Identification using machine learning algorithms. **A** Lasso regression was used to screen the key genes of GSE73680, with the optimal gene count ($n=7$) at the curve's lowest point. **B**-**C** Core genes were screened by Boruta algorithm, and a total of 2 genes were screened. **D** Lasso regression was used to screen the key genes of GSE56815, with the optimal gene count ($n=10$) at the curve's lowest point. **E**–**F** Core genes were screened by Boruta algorithm, and a total of 9 genes were screened. **G** Common genes identified by the two algorithms

algorithms in a joint analysis. This approach led to the identification of AKT1 and TNF as the most prominent core targets (Fig. 5C-I). These targets, together with the core genes identified in the previous machine learning analysis, were then used for drug prediction.

GeneMANIA-based functional association

The Protein–Protein Interaction (PPI) network constructed using GeneMANIA (https://genemania.org/) included 20 additional genes that could potentially interact with the three core targets we identified, in addition to the three core targets themselves (Fig. 6A). These interactions comprised Physical Interactions (77.64%), Co-expression (8.01%), and other types. Functional analysis of the network highlighted the roles of the drug targets and related genes, as well as their functions. The results revealed correlations with exogenous apoptotic signaling pathways and the modulation of inflammatory responses, demonstrating a strong functional connection between immunity and inflammation, consistent with the pathogenesis of osteoporosis and kidney stones. The GMFA approach integrates co-expression, genetic interactions, and physical

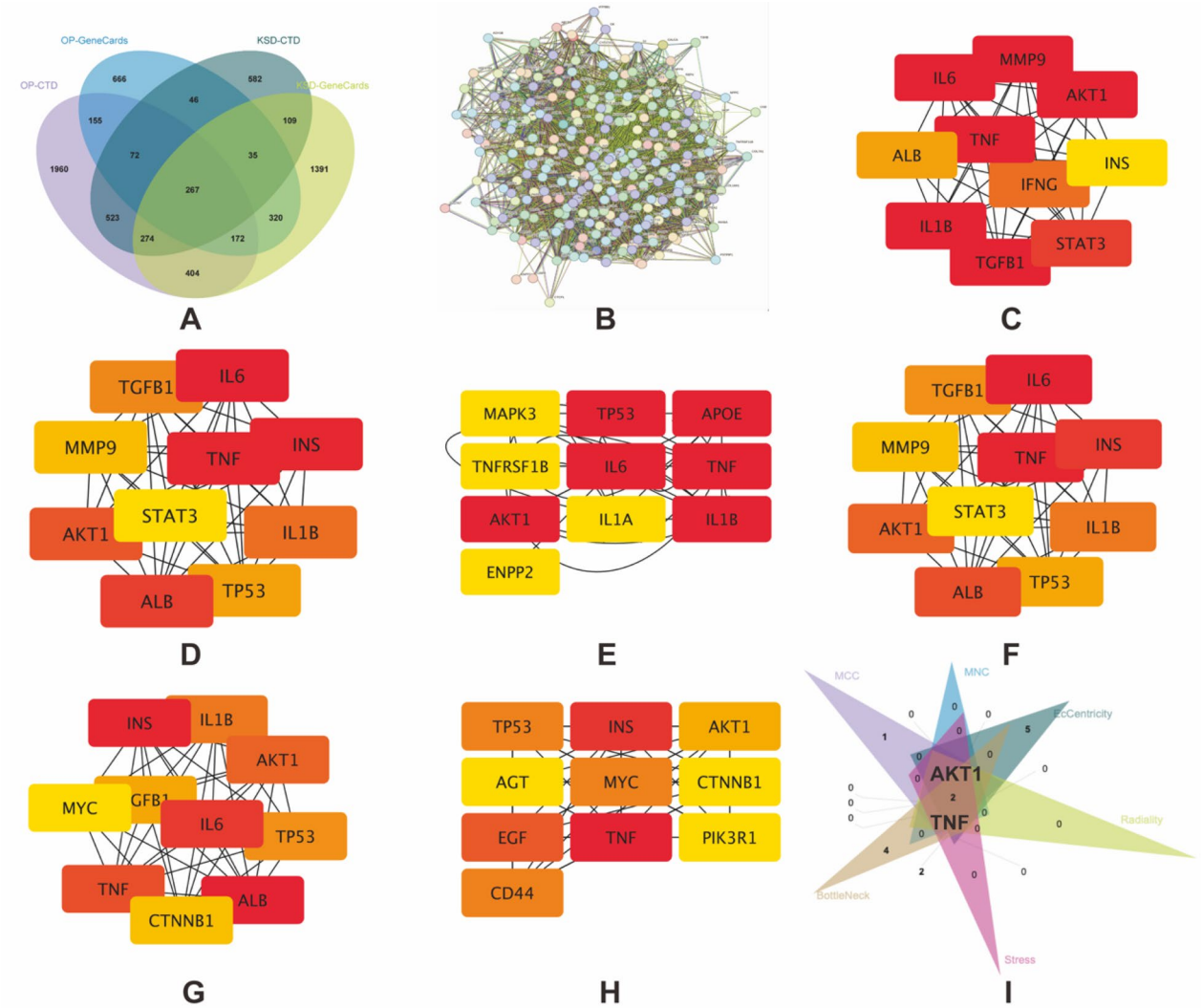

Fig. 5 Shared genes were screened based on public databases. **A** Venn diagram of interaction between common targets and genes from CTD and GeneCards analysis. **B** The PPI network and clusters analysis of common targets. **C**-**H** The top 10 core genes were sequentially calculated by MCC, MNC, Radiality, Stress, BottleNeck and EcCentricity algorithms. **I** The key targets obtained were comprehensively analyzed

interactions to capture a wide array of genes associated with disease [14]. In subsequent KEGG enrichment analysis, GMFA identified the mTOR signaling pathway as the most significant pathway in the shared mechanism (Fig. 6B).

Analysis of immune cell infiltration

To investigate the pathogenesis of Alzheimer's disease (AD) and ankylosing spondylitis (AS), we examined immune cell infiltration patterns in patient tissues. Using the CIBERSORT algorithm, we obtained infiltration scores for various immune cell types. Analysis of the GSE73680 dataset revealed a significantly higher infiltration of resting dendritic cells and M1 macrophages, as well as a significantly lower infiltration of resting mast cells in the KSD group compared to the normal group (Fig. 7A-C). In contrast, the OP dataset, which detected mononuclear cells, showed no significant differences in immune cell infiltration between the normal and osteoporosis groups, further confirming the reliability of our study (Fig. 7D-F).

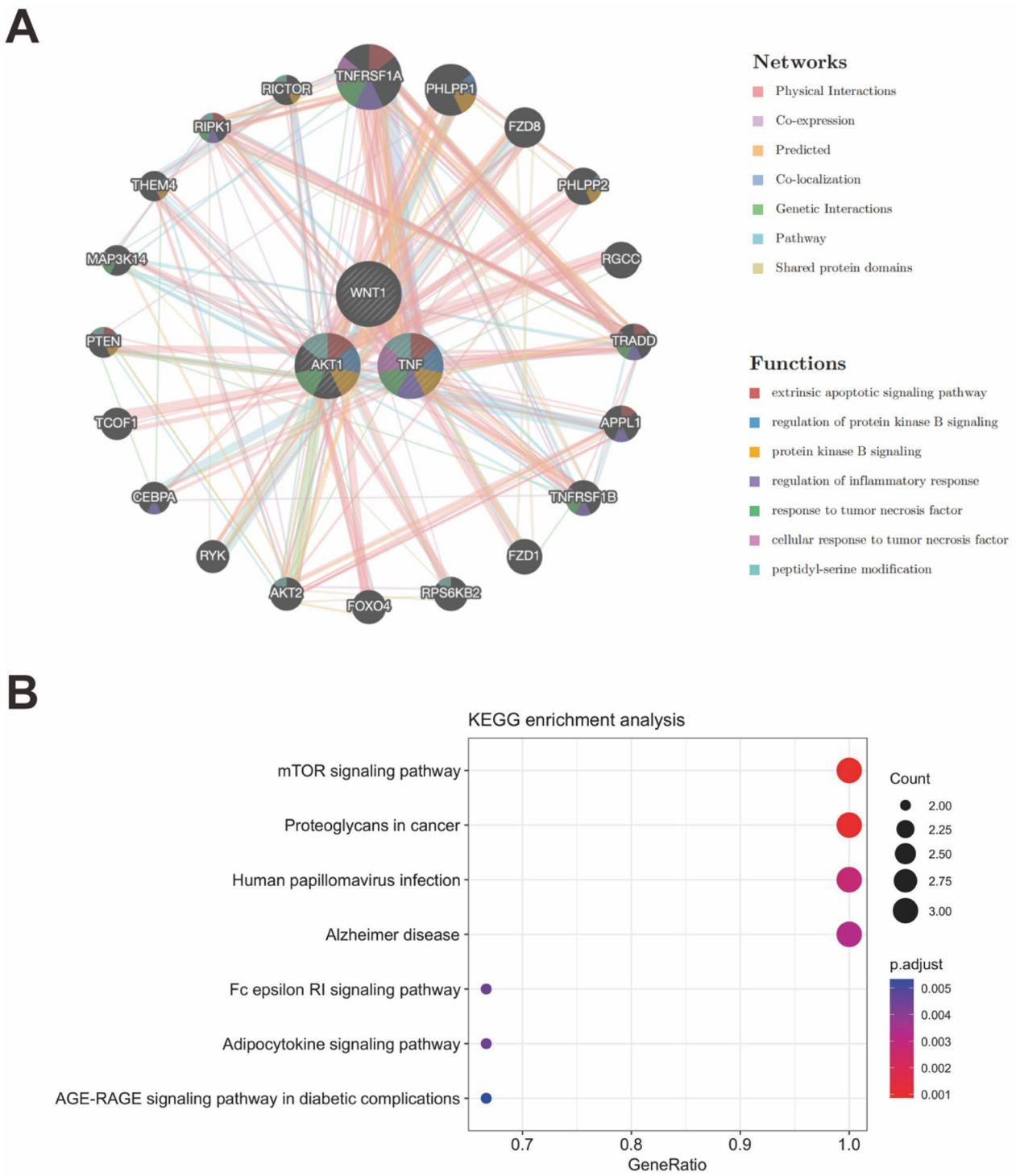

Fig. 6 GeneMANIA functional association (GMFA) network analysis. **A** PPI network built with GeneMANIA. Each circle is coloured to indicate the functional pathway in which each gene is involved. **B** KEGG enrichment analysis

Candidate drug prediction

In this study, we employed DSigDB to predict potential therapeutic interventions. Based on our screening results and a review of the literature, we identified nine drugs that may offer potential for allopathic treatment. These include butein, diosgenin, tylophorine, garcinol,

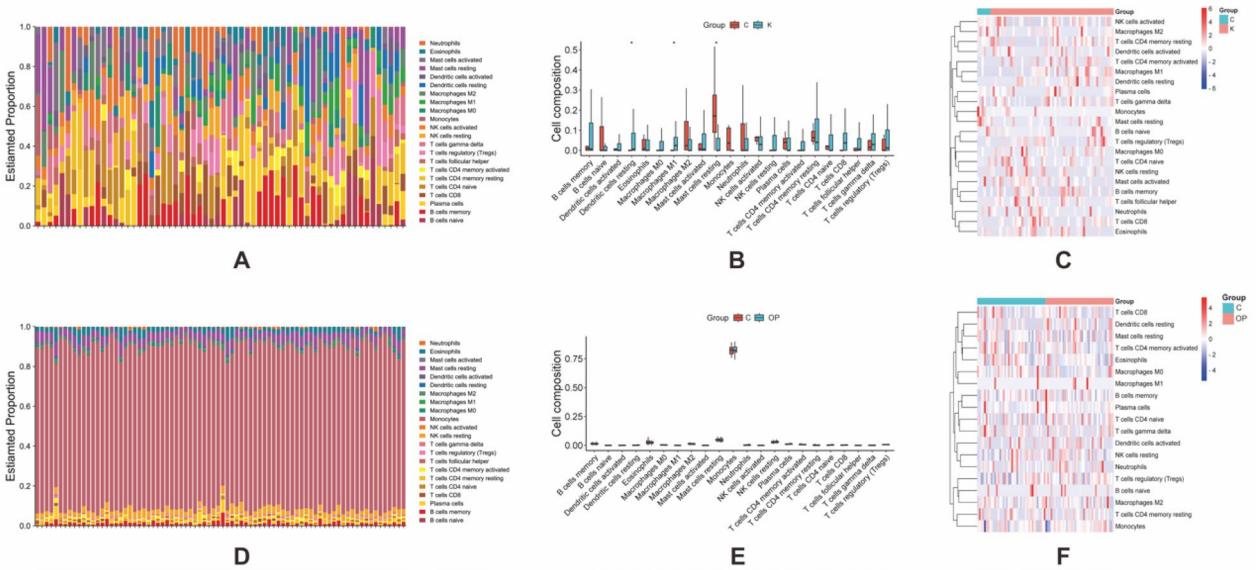

Fig. 7 Immune cell infiltration analysis of KSD and OP. **A**-**C** Analysis of the proportions of various immune cell infiltrates in GSE73680 using the CIBERSORT algorithm. **D**-**F** Analysis of the proportions of various immune cell infiltrates in GSE56815 using the CIBERSORT algorithm

sphingosine 1-phosphate, evodiamine, linalool, cilostazol, and naringenin (Table 4). Most of these drugs possess anti-inflammatory, antioxidant, and hormone-modulating properties, which align with the pathogenesis of osteoporosis and kidney stones, as well as their comorbidity.

Molecular docking

To evaluate the affinity of drug candidates for their targets and assess the druggability of these targets, molecular docking was conducted in this study. The CB-Dock2 platform was used to identify the binding sites and interactions of nine drug candidates with their respective target proteins. For each interaction, we calculated the binding energy, resulting in a total of 18 successful docking outcomes between the proteins and drugs (Fig. 8A-R and Supplementary Table 2). In this analysis, we found that Evodiamine exhibited the most stable binding to AKT1, cilostazol also bound stably to AKT1, and diosgenin showed stable binding to TNF, with binding energies of −10 kcal/mol, −10.7 kcal/mol, and −10.2 kcal/mol, respectively.

Discussion

In this study, we conducted a cross-sectional analysis of nationally representative NHANES data to examine the association between osteoporosis/bone loss and kidney stones. Our findings indicate that individuals with kidney stones exhibit lower femoral neck and lumbar spine bone mineral density (BMD) and have a higher prevalence of osteoporosis compared to those without kidney stones. Mechanistic investigations revealed that the mTOR signaling pathway is a key shared mechanism underlying both osteoporosis and kidney stones. Additionally, the following compounds—butein, diosgenin, tylophorine, garcinol, sphingosine 1-phosphate, evodiamine, linalool, cilostazol, and naringenin—may serve as potential therapeutic agents targeting this association.

Studies have demonstrated that individuals with metabolic bone disease are at a higher risk of developing kidney stones [24, 25]. Shared risk factors for both osteoporosis and kidney stones, such as physical inactivity, may contribute to the increased risk of kidney stones in patients with osteoporosis [26]. Additionally, comorbidities can heighten susceptibility to both conditions. In patients with ankylosing spondylitis, low bone mineral density (BMD) is associated with the presence of kidney stones [27]. Reduced BMD and elevated bone resorption markers can collectively influence the risk of multi-organ calcification. Specifically, low BMD and increased bone resorption are linked to mitral valve calcification and kidney stones [28]. Our adjusted multifactorial logistic regression analysis revealed that decreased femoral neck and lumbar spine BMD were associated with a higher risk of kidney stones, a finding that remained consistent after stratification by sex. Similarly, Kim et al. used stratified Cox proportional hazards modeling to examine the impact of osteoporosis on the National Health Service health screening cohort (2002–2015) in individuals

Table 4 Candidate drug predicted using DSigDB

Drug names	Constitutional formula	Clinical applications or potential	Mechanism of action	*P* value	Genes
Butein CTD 00001872	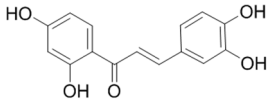	Anticancer effect, anti-inflammatory effect, antioxidant effect	Butein Activates Autophagy Through AMPK/TSC2/ULK1/mTOR Pathway to Inhibit IL-6 Expression in IL-1β Stimulated Human Chondrocytes [15]	8.25E−07	AKT1; TNF
DIOSGENIN CTD 00005850	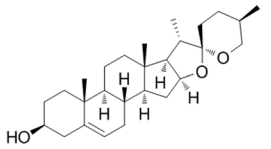	Immunomodulation, antitumor effect, neuroprotective effect, cardiovascular protection	Diosgenin attenuates nonalcoholic fatty liver disease through mTOR-mediated inhibition of lipid accumulation and inflammation [16]	1.57E−06	AKT1; TNF
Tylophorine CTD 00000134	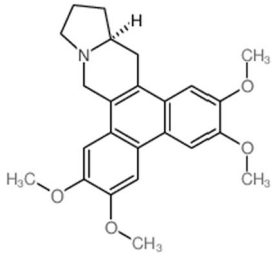	Anti-cancer treatment, anti-inflammatory treatment, anti-asthma treatment, antibacterial treatment	A novel tylophorine analog W-8 up-regulates forkhead boxP3 expression and ameliorates murine colitis [17]	2.29E−06	AKT1; TNF
Garcinol CTD 00002324	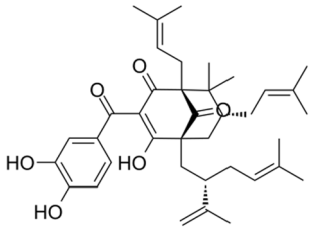	Cancer treatment, inflammatory disease treatment	Garcinol-Attenuated Gastric Ulcer (GU) Experimentally Induced in Rats Via Affecting Inflammation, Cell Proliferation, and DNA Polymerization [18]	3.46E−06	AKT1; TNF
Sphingosine 1-phosphate CTD 00002508	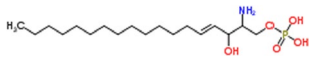	Cancer treatment, cardiovascular treatment, neuroprotection, immunomodulation	Sphingosine-1-phosphate induces myocyte autophagy after myocardial infarction through mTOR inhibition [19]	4.50E−06	AKT1; TNF
Evodiamine CTD 00002158	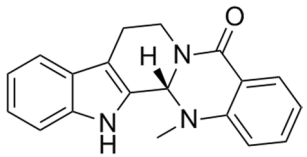	Anti-cancer effect, weight loss effect, anti-inflammatory effect, blood pressure reduction effect	Induction of Apoptosis and Effect on the FAK/AKT/mTOR Signal Pathway by Evodiamine in Gastric Cancer Cells [20]	5.26E−06	AKT1; TNF

Table 4 (continued)

Drug names	Constitutional formula	Clinical applications or potential	Mechanism of action	*P* value	Genes
Linalool CTD 00000957	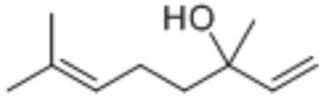	Antineoplastic effect, nervous system regulation, antioxidant effect	Linalool induces cell cycle arrest and apoptosis in HepG2 cells through oxidative stress generation and modulation of Ras/MAPK and Akt/mTOR pathways [21]	9.44E−06	AKT1; WNT1
Cilostazol CTD 00002032	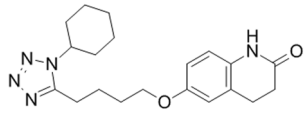	Treatment of intermittent claudication, prevention of cerebral infarction recurrence, prevention of stent restenosis and thrombosis after PCI, anti-atherosclerosis	Cilostazol novel neuroprotective mechanism against rotenone-induced Parkinson's disease in rats: Correlation between Nrf2 and HMGB1/TLR4/PI3K/Akt/mTOR signaling [22]	1.17E−05	AKT1; TNF
Naringenin CTD 00000211	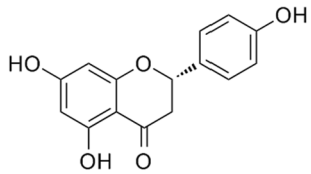	Antioxidant effect, anti-cancer effect, anti-inflammatory effect, regulation of lipid metabolism	Naringenin alleviate reproductive toxicity evoked by lead acetate via attenuation of sperm profile and biochemical alterations in male Wistar rat: Involvement of TGFβ/AKT/mTOR pathway [23]	1.29E−05	AKT1; TNF

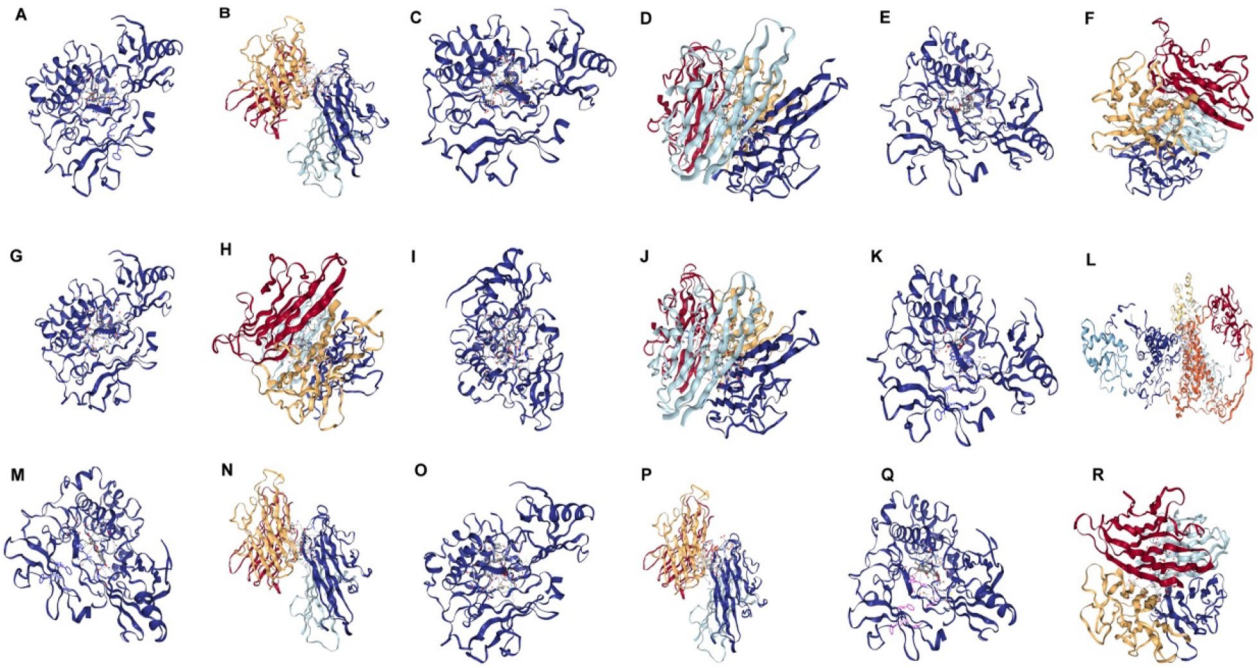

Fig. 8 Docking results of available proteins small molecules. **A** AKT1 docking butein. **B** TNF docking butein. **C** AKT1 docking cilostazol. **D** TNF docking cilostazol. **E** AKT1 docking diosgenin. **F** TNF docking diosgenin. **G** AKT1 docking evodiamine. **H** TNF docking evodiamine. **I** AKT1 docking garcinol. **J** TNF docking garcinol garcinol. **K** AKT1 docking linalool. **L** WNT1 docking linalool. **M** AKT1 docking naringenin. **N** TNF docking naringenin. **O** AKT1 docking sphingosine 1-phosphate. **P** TNF docking sphingosine 1-phosphate. **Q** AKT1 docking tylophorine. **R** TNF docking tylophorine

over 40 years of age. Their analysis showed that the hazard ratio (HR) for kidney stones in patients with osteoporosis was 1.36 times higher than in controls (95% CI 1.28–1.45) [24]. This result aligns with our findings from multifactorial logistic regression analysis (Model 3), which showed that osteoporotic patients (OR = 1.41; 95% CI = 1.11–1.79, $P = 0.005$) had a significantly higher incidence of kidney stones.

mTOR is an atypical serine/threonine protein kinase that integrates upstream signaling with downstream effectors, including transcription and translation, to regulate essential cellular processes such as energy utilization, protein synthesis, autophagy, cell growth, and proliferation [29]. The mTOR signaling pathway plays a crucial role in bone metabolism by regulating osteoblast proliferation, differentiation, autophagy, survival, and apoptosis, thereby significantly influencing bone mass [30, 31]. Specifically: Regulation of Bone Metabolism through Osteoblast Autophagy: The mTOR signaling pathway can inhibit autophagy, the cellular process responsible for degrading damaged or excess proteins and organelles. In osteoblasts, mTOR inhibition enhances autophagy, reducing bone resorption and improving bone quality. Regulation of Bone Metabolism through Osteoblast Maturation and Differentiation: mTORC2, a key regulator of osteoblast maturation, promotes the proliferation and activity of osteoblasts, thereby improving bone quality and density. Regulation of Bone Metabolism through Osteoblast Survival and Apoptosis: mTORC1 can induce osteoblast apoptosis, while mTORC2 enhances osteoblast survival by inhibiting acylated proteases. Drugs specifically targeting the mTOR signaling pathway have the potential to emerge as a novel therapeutic strategy for osteoporosis. For instance, the application of mTORC1 inhibitors can effectively quell the proliferation and differentiation of osteocytes, consequently diminishing bone resorption. This, in turn, leads to an augmentation in bone density and bone mass, thereby enhancing the stability of bone tissue. By finely tuning the mTOR signaling pathway, the differentiation and activity of osteoblasts can be encouraged, further bolstering bone quality and bone mineral density. This approach offers osteoporosis patients a fresh alternative in their treatment options.

The mTOR signaling pathway is a crucial intracellular pathway that regulates cell division, gene transcription, and protein translation, primarily through the activation of the PI3K/Akt/mTOR axis. This pathway controls protein synthesis, thereby influencing cell growth [32]. Inhibition of the mTOR signaling pathway can effectively disrupt abnormal signaling triggered by various growth factors, thereby preventing excessive cell proliferation and metabolic activity, which is critical for reducing

renal stone formation [33, 34]. Regulation of Cellular Metabolism: Inhibition of the mTOR pathway lowers cellular metabolic activity, reducing the production and deposition of crystalline substances in the urine. By modulating the metabolic processes of renal tubular epithelial cells, mTOR inhibition reduces the oversaturation of crystalline substances, such as calcium oxalate, thereby decreasing the risk of kidney stone formation. Influence on Cell Proliferation and Differentiation: The mTOR pathway plays a vital role in regulating cell proliferation and differentiation. Its inhibition slows the proliferation of renal tubular epithelial cells and decreases the likelihood of their differentiation into cell types involved in stone formation. This reduction in abnormal cell numbers and activity helps mitigate kidney stone formation. Regulation of Inflammatory Response [35]: Kidney stone formation is frequently accompanied by inflammation. Inhibiting the mTOR pathway reduces the inflammatory response in renal tubular epithelial cells and lowers the release of inflammatory mediators. This helps prevent damage to renal tissues and reduces both the formation and recurrence of kidney stones. Promotion of Cellular Autophagy: As a major negative regulator of autophagy, the mTOR pathway inhibits this process. By blocking mTOR signaling, autophagy is enhanced in renal tubular epithelial cells, enabling them to remove damaged or excess proteins and organelles. This process helps maintain intracellular homeostasis and reduces the deposition of crystalline material, thereby lowering the risk of kidney stone formation. Drugs targeting the mTOR signaling pathway may help to reduce the deposition of urinary salt crystals and damage to renal tubular epithelial cells, thereby preventing or treating kidney stones. By regulating mTOR signaling pathway, it can improve the metabolism and function of renal tubular epithelial cells, reduce the formation and retention of urinary salt crystals, and provide a new treatment for patients with kidney stones.

Potential clinical translation value summary, drug development: Drug development targeting mTOR signaling pathway may provide new options for the treatment of osteoporosis and kidney stones. These drugs can exert therapeutic effects by regulating the mTOR signaling pathway to affect bone metabolism and urinary salt crystal formation. Personalized treatment: By detecting the activity of mTOR signaling pathway in patients, personalized treatment plans can be provided for patients. For example, in patients with osteoporosis, if reduced activity of the mTOR signaling pathway is detected, drugs that promote mTOR activity can be considered to increase bone formation; For patients with kidney stones, if excessive mTOR signaling activity is detected, drugs that inhibit mTOR activity may be considered to reduce the formation of urinary salt crystals. Combination therapy: There are complex interactions between mTOR signaling and other signaling pathways. Therefore, the combination of drugs targeting mTOR signaling pathway with other drugs may produce better therapeutic effects. For example, in the treatment of osteoporosis, drugs that promote mTOR activity can be combined with drugs that promote osteoblast differentiation; In the treatment of kidney stones, drugs that inhibit mTOR activity can be combined with drugs that promote urinary salt excretion.

Butein, diosgenin, tylophorine, garcinol, sphingosine 1-phosphate, evodiamine, and linalool are natural products or compounds with significant biological activities, making them potential candidates for drug development and medicinal applications. Butein has been shown to suppress the proliferation and survival of tumor cells by inhibiting the activity of mTORC1, thereby modulating the phosphorylation levels of its downstream target proteins, such as 4E-BP1 and p70S6K [15, 36]. Diosgenin, on the other hand, exerts its effects by inhibiting PI3K activity, which subsequently reduces the production of PIP3 and inhibits AKT phosphorylation. Given that AKT is a key activator of mTORC1, the inhibition of AKT by Diosgenin indirectly suppresses mTORC1 activity, ultimately leading to decreased cell proliferation and increased apoptosis [16]. Tylophorine may also inhibit mTORC1 activity, affecting the expression of cyclin D1 and E, and thereby arresting the cell cycle progression and inhibiting tumor cell proliferation [17]. Garcinol has been found to reduce inflammatory responses by inhibiting the TLR4/NF-κB signaling pathway, thereby decreasing the production of inflammatory factors. Since there is cross-talk between inflammatory signaling and the mTOR pathway, Garcinol's anti-inflammatory effects may indirectly influence the mTOR signaling pathway [18]. Sphingosine 1-phosphate (S1P) can activate the PI3K/AKT pathway through its receptor S1PR1, which in turn activates mTORC1. Additionally, S1P may affect mTORC2 activity through other mechanisms, either directly or indirectly [37]. Evodiamine inhibits FAK activity, leading to reduced AKT phosphorylation and subsequent inhibition of the mTOR signaling pathway. Furthermore, Evodiamine may also influence the activity of mTORC1 and mTORC2 through other mechanisms [20]. Linalool, with its antioxidant properties, may reduce cellular oxidative stress levels, thereby affecting the mTOR signaling pathway. Given that oxidative stress is a significant regulator of the mTOR pathway, Linalool's antioxidant effects may indirectly modulate mTOR signaling [21]. These compounds exhibit a range of biological activities, including anticancer, antibacterial, anti-inflammatory, and neuroprotective effects, and could play a role in the heterogeneous treatment of osteoporosis and kidney stones [36–42]. mTOR signaling pathway plays an important role in the

pathogenesis of osteoporosis and kidney stones. By regulating this pathway, some natural compounds and traditional Chinese medicine monomers may provide new strategies for the treatment of related diseases. However, the specific mechanisms of action and clinical applications of these compounds need to be further investigated.

The primary strength of this study lies in the integration of data from NHANES, GEO, CTD, and GeneCards. The comprehensive evaluation of various factors, coupled with the large sample size, enabled us to effectively adjust for multiple confounders in multivariate regression models, thereby providing sufficient statistical power to investigate the pathogenic associations between BMD, osteoporosis, and kidney stones. Additionally, the study contributes to a deeper understanding of biological connections by exploring the shared molecular mechanisms underlying these conditions.

However, several limitations must be acknowledged. Firstly, excluding participants with missing data could introduce potential bias, typically categorized as missing-not-at-random (MNAR), which may further result in selection bias. To mitigate this, we meticulously designed the study to anticipate missing data and employed multiple imputation techniques to handle such instances. Additionally, self-reported data from questionnaires are prone to recall bias. Future studies could address this limitation by supplementing self-reported data with objective measures, such as biomarkers or direct observations, to provide a more comprehensive understanding of the associations under investigation. Secondly, despite controlling for numerous relevant covariates, residual and unmeasured confounders may still influence the results. Thirdly, our findings primarily reflect the European American population, which limits the generalizability of our conclusions to other ethnic groups. To enhance the generalizability of future studies, it is crucial to include participants from diverse racial and ethnic backgrounds. This would provide a broader perspective and enable more inclusive conclusions regarding the associations studied. Future studies with larger, more diverse sample populations are necessary to validate our results. Lastly, while the underlying mechanisms of renal stone formation vary according to different stone compositions, the lack of data on stone composition in the NHANES dataset may have compromised the reliability of our findings. The absence of detailed information on stone composition limits the interpretation of findings related to kidney stones. Different types of kidney stones (e.g., calcium oxalate, uric acid) may have distinct underlying causes and management strategies. Future studies should aim to collect comprehensive data on stone composition, which will allow for a more nuanced analysis and may identify specific risk factors associated with different types of stones. Therefore, further well-designed prospective studies, along with investigations into the biological mechanisms, are essential to uncover the complex links between osteoporosis/osteopenia and kidney stones. Such research will provide a scientific foundation for early disease diagnosis, personalized treatment strategies, and the development of preventive measures. Moreover, it will enhance our understanding of the pathophysiological interactions between the skeletal and urinary systems and promote advancements in both basic research and clinical applications in these fields.

Conclusions

Bone loss is associated with an increased risk of kidney stones. Targeting the mTOR signaling pathway may offer a potential therapeutic approach for treating both osteoporosis and kidney stones.

Abbreviations

KSD	Kidney stone disease
NHANES	National health and nutrition examination survey
BMD	Bone mineral density
FN BMD	Femoral neck bone mineral density
LS BMD	Lumbar spine bone mineral density
DXA	Dual-energy X-ray absorptiometry
SD	Standard deviations
BMI	Body mass index
DEG	Differential gene expression
DEGs	Differentially expressed genes
PPI	Protein–protein interaction
DSigDB	Drug signature database
OR	Odds ratios
CI	Confidence intervals
RCS	Restricted cubic spline
OP	Osteoporosis
HR	Hazard ratio
ALP	Alkaline phosphatase

Supplementary Information

The online version contains supplementary material available at https://doi.org/10.1186/s13062-025-00627-w.

Supplementary Material 1

Acknowledgements

We thank all the participants involved in this study. We thank NHANES database, GEO database, CTD database, GeneCards database and DSigDB database for allowing us to use their data.

Author contributions

LD: protocol/project development, data collection and management, data analysis, and manuscript writing; XLG and ZJD: protocol/project development and manuscript editing; LD and LCY: protocol/project development, data collection and management, data analysis, and manuscript writing. All authors have read and agreed to the published version of the manuscript.

Funding

Clinical Medical Research Program, The Second Hospital of Tianjin Medical University(2023LC01) and (2023HK025).

Data availability

The datasets used and/or analyzed during the current study are available from the corresponding author on reasonable request.

Declarations

Ethics approval and consent to participate
All studies providing data for these analyses have been approved by the relevant Institutional Review Boards of each country, and the Institutional Review Board of the Second Hospital of Tianjin Medical University is in accordance with the Declaration of Helsinki.

Consent for publication
Not applicable.

Competing interests
The authors declare no competing interests.

Received: 14 December 2024 Accepted: 5 March 2025
Published online: 31 March 2025

References

1. Rachner TD, Khosla S, Hofbauer LC. Osteoporosis: now and the future. Lancet. 2011;377(9773):1276–87.
2. Khan SR, Pearle MS, Robertson WG, Gambaro G, Canales BK, Doizi S, Traxer O, Tiselius HG. Kidney stones. Nat Rev Dis Primers. 2016;2:16008.
3. Ebeling PR, Nguyen HH, Aleksova J, Vincent AJ, Wong P, Milat F. Secondary osteoporosis. Endocr Rev. 2022;43(2):240–313.
4. Gallagher JC, Rosen CJ. Vitamin D: 100 years of discoveries, yet controversy continues. Lancet Diabetes Endocrinol. 2023;11(5):362–74.
5. Peerapen P, Thongboonkerd V. Kidney stone prevention. Adv Nutr. 2023;14(3):555–69.
6. Howles SA, Thakker RV. Genetics of kidney stone disease. Nat Rev Urol. 2020;17(7):407–21.
7. Prochaska M, Taylor E, Vaidya A, Curhan G. Low bone density and bisphosphonate use and the risk of kidney stones. Clin J Am Soc Nephrol. 2017;12(8):1284–90.
8. Zhang S, Huang X, Zhao X, Li B, Cai Y, Liang X, Wan Q. Effect of exercise on bone mineral density among patients with osteoporosis and osteopenia: a systematic review and network meta-analysis. J Clin Nurs. 2022;31(15–16):2100–11.
9. Xiao Y, Wang J, Yin S, Tang Y, Cui J, Yang Z, Huang K, Wang J, Bai Y. Association between physical activity and the prevalence of kidney stones in American adults: results from a multiyear national survey. Urology. 2024;189:9–18.
10. Dang K, Wang X, Hu J, Zhang Y, Cheng L, Qi X, Liu L, Ming Z, Tao X, Li Y. The association between triglyceride-glucose index and its combination with obesity indicators and cardiovascular disease: NHANES 2003–2018. Cardiovasc Diabetol. 2024;23(1):8.
11. Li Y, Di X, Liu M, Wei J, Li T, Liao B. Association between daily sitting time and kidney stones based on the national health and nutrition examination survey (NHANES) 2007–2016: a cross-sectional study. Int J Surg. 2024;110(8):4624–32.
12. Looker AC, Orwoll ES, Johnston CC Jr, Lindsay RL, Wahner HW, Dunn WL, Calvo MS, Harris TB, Heyse SP. Prevalence of low femoral bone density in older U.S. adults from NHANES III. J Bone Miner Res. 1997;12(11):1761–8.
13. Hou W, Chen S, Zhu C, Gu Y, Zhu L, Zhou Z. Associations between smoke exposure and osteoporosis or osteopenia in a US NHANES population of elderly individuals. Front Endocrinol (Lausanne). 2023;14:1074574.
14. Rajadnya R, Sharma N, Mahajan A, Ulhe A, Patil R, Hegde M, Mali A. Novel systems biology experimental pipeline reveals matairesinol's antimetastatic potential in prostate cancer: an integrated approach of network pharmacology, bioinformatics, and experimental validation. Brief Bioinform. 2024;25(5):466.
15. Ansari MY, Ahmad N, Haqqi TM. Butein activates autophagy through AMPK/TSC2/ULK1/mTOR pathway to inhibit IL-6 expression in IL-1β stimulated human chondrocytes. Cell Physiol Biochem. 2018;49(3):932–46.
16. Yin G, Liang H, Cheng Y, Chen S, Zhang X, Meng D, Yu W, Liu H, Song C, Zhang F. Diosgenin attenuates nonalcoholic fatty liver disease through mTOR-mediated inhibition of lipid accumulation and inflammation. Chem Biol Interact. 2025;405:111306.
17. Meng X, Zhang Y, Jia Z, Huo X, He X, Tian G, Wu M, Wang Z, Zhou X, Xiong S, et al. A novel tylophorine analog W-8 up-regulates forkhead boxP3 expression and ameliorates murine colitis. J Leukoc Biol. 2013;93(1):83–93.
18. Alatawi YF, Alhablani MA, Al-Rashidi FA, Khubrani WS, Alqaisi SA, Hassan HM, Al-Gayyar MM. Garcinol-attenuated gastric ulcer (GU) experimentally induced in rats via affecting inflammation, cell proliferation, and DNA polymerization. Cureus. 2023;15(8):e43317.
19. Yang LG, Wang AL, Li L, Yang H, Jie X, Zhu ZF, Zhang XJ, Zhao HP, Chi RF, Li B, et al. Sphingosine-1-phosphate induces myocyte autophagy after myocardial infarction through mTOR inhibition. Eur J Pharmacol. 2021;907:174260.
20. Yang JY, Woo HJ, Lee P, Kim SH. Induction of apoptosis and effect on the FAK/AKT/mTOR signal pathway by evodiamine in gastric cancer cells. Curr Issues Mol Biol. 2022;44(9):4339–49.
21. Rodenak-Kladniew B, Castro A, Stärkel P, De Saeger C, García de Bravo M, Crespo R. Linalool induces cell cycle arrest and apoptosis in HepG2 cells through oxidative stress generation and modulation of Ras/MAPK and Akt/mTOR pathways. Life Sci. 2018;199:48–59.
22. El-Sayed RM, Abdelaziz AM, Zaki HF, Abdel Rasheed NO. Cilostazol novel neuroprotective mechanism against rotenone-induced Parkinson's disease in rats: correlation between Nrf2 and HMGB1/TLR4/PI3K/Akt/mTOR signaling. Int Immunopharmacol. 2023;117:109986.
23. Elhemiely AA, Yahia R, Gad AM. Naringenin alleviate reproductive toxicity evoked by lead acetate via attenuation of sperm profile and biochemical alterations in male Wistar rat: involvement of TGFβ/AKT/mTOR pathway. J Biochem Mol Toxicol. 2023;37(6):e23335.
24. Kim SY, Chung J, Park DS, Yoo DM, Bang WJ, Choi HG. The reciprocal relationship between osteoporosis and renal stones. J Clin Med. 2022;11(22):6614.
25. Jia S, Liao J, Wang Y, Zheng W, Jin J, Xu W, Zheng Q. Prevalence of osteoporosis in patients with nephrolithiasis and vice versa: a cumulative analysis. Front Endocrinol (Lausanne). 2023;14:1180183.
26. Reid LJ, Muthukrishnan B, Patel D, Seckl JR, Gibb FW. Predictors of nephrolithiasis, osteoporosis, and mortality in primary hyperparathyroidism. J Clin Endocrinol Metab. 2019;104(9):3692–700.
27. Incel NA, Gökoğlu F, Nacir B, Incel N. Bone and stone in ankylosing spondylitis: osteoporosis and urolithiasis. Clin Rheumatol. 2006;25(5):667–70.
28. Celik A, Davutoglu V, Sarica K, Erturhan S, Ozer O, Sari I, Yilmaz M, Baltaci Y, Akcay M, Al B, et al. Relationship between renal stone formation, mitral annular calcification and bone resorption markers. Ann Saudi Med. 2010;30(4):301–5.
29. Marques-Ramos A, Cervantes R. Expression of mTOR in normal and pathological conditions. Mol Cancer. 2023;22(1):112.
30. Xian L, Wu X, Pang L, Lou M, Rosen CJ, Qiu T, Crane J, Frassica F, Zhang L, Rodriguez JP, et al. Matrix IGF-1 maintains bone mass by activation of mTOR in mesenchymal stem cells. Nat Med. 2012;18(7):1095–101.
31. Wang S, Deng Z, Ma Y, Jin J, Qi F, Li S, Liu C, Lyu FJ, Zheng Q. The role of autophagy and mitophagy in bone metabolic disorders. Int J Biol Sci. 2020;16(14):2675–91.
32. Glaviano A, Foo ASC, Lam HY, Yap KCH, Jacot W, Jones RH, Eng H, Nair MG, Makvandi P, Geoerger B, et al. PI3K/AKT/mTOR signaling transduction pathway and targeted therapies in cancer. Mol Cancer. 2023;22(1):138.
33. Unno R, Kawabata T, Taguchi K, Sugino T, Hamamoto S, Ando R, Okada A, Kohri K, Yoshimori T, Yasui T. Deregulated MTOR (mechanistic target of rapamycin kinase) is responsible for autophagy defects exacerbating kidney stone development. Autophagy. 2020;16(4):709–23.
34. Sun Y, Dai S, Tao J, Li Y, He Z, Liu Q, Zhao J, Deng Y, Kang J, Zhang X, et al. Taurine suppresses ROS-dependent autophagy via activating Akt/mTOR signaling pathway in calcium oxalate crystals-induced renal tubular epithelial cell injury. Aging (Albany NY). 2020;12(17):17353–66.
35. Wang J, Zhang Y, Cao J, Wang Y, Anwar N, Zhang Z, Zhang D, Ma Y, Xiao Y, Xiao L, et al. The role of autophagy in bone metabolism and clinical significance. Autophagy. 2023;19(9):2409–27.
36. Behera BP, Mishra SR, Mahapatra KK, Patil S, Efferth T, Bhutia SK. SIRT1-activating butein inhibits arecoline-induced mitochondrial dysfunction through PGC1α and MTP18 in oral cancer. Phytomedicine. 2024;129:155511.

37. Cartier A, Hla T. Sphingosine 1-phosphate: lipid signaling in pathology and therapy. Science. 2019;366(6463):5551.
38. Yan M, Zhao Y, Man S, Dai Y, Ma L, Gao W. Diosgenin as a substitute for cholesterol alleviates NAFLD by affecting CYP7A1 and NPC1L1-related pathway. Phytomedicine. 2024;125:155299.
39. Kausar MA, Parveen S, Anwar S, Sadaf S, Massey S, El-Horany HE, Khan FH, Shahein M, Husain SA. Cytotoxic potential and metabolomic profiling of alkaloid rich fraction of *Tylophora indica* leaves. Biochim Biophys Acta Mol Cell Biol Lipids. 2024;1869(6):159505.
40. Zou J, Chen H, Fan X, Qiu Z, Zhang J, Sun J. Garcinol prevents oxidative stress-induced bone loss and dysfunction of BMSCs through NRF2-antioxidant signaling. Cell Death Discov. 2024;10(1):82.
41. Chen S, Bi K, Liang H, Wu Z, Huang M, Chen X, Dong G, Sheng C. PROTAC derivatization of natural products for target identification and drug discovery: design of evodiamine-based PROTACs as novel REXO4 degraders. J Adv Res. 2024;63:219–30.
42. Chang WH, Hsu HT, Lin CC, An LM, Lee CH, Ko HH, Lin CL, Lo YC. Linalool, a fragrance compound in plants, protects dopaminergic neurons and improves motor function and skeletal muscle strength in experimental models of parkinson's disease. Int J Mol Sci. 2024;25(5):2514.

Publisher's Note